Biochemistry

 Volume 41, Number 35 September 3, 2002

Accelerated Publications

Substrate Binding Induces a Cooperative Conformational Change in the 12S Subunit of Transcarboxylase: Raman Crystallographic Evidence†

Xiaojing Zheng,‡ Rosa E. Rivera-Hainaj,‡ Yuangang Zheng,‡ Marianne Pusztai-Carey,‡ Pamela R. Hall,§ Vivien C. Yee,§ and Paul R. Carey*,‡

Department of Biochemistry and Department of Pharmacology, Case Western Reserve University, Cleveland, Ohio 44106, and Department of Molecular Cardiology and Center for Structural Biology, Learner Research Institute, Cleveland Clinic Foundation, 9500 Euclid Avenue NB20, Cleveland, Ohio 44195

Received June 18, 2002; Revised Manuscript Received July 16, 2002

ABSTRACT: The 12S subunit of transcarboxylase is a 338 000 Da hexamer that transfers carboxylate from methylmalonyl-CoA (MM-CoA) to biotin; in turn, the biotin transfers the carboxylate to pyruvate on another subunit, the 5S. Here, Raman difference microscopy is used to study the binding of substrate and product, and their analogues, to single crystals of 12S. A single crystal is the medium of choice because it provides Raman data of unprecedented quality. Crystalline ligand−protein complexes were formed by cocrystallization or by the soaking in/soaking out method. Raman difference spectra were obtained by subtracting the spectrum of the apo crystal from that of a crystal with the substrate or product bound. Raman difference spectra from crystals with the substrate bound are dominated by bands from the protein's amide bonds and aromatic side chain residues. In contrast, Raman difference spectra involving the product, propionyl-CoA, are dominated by modes from the ligand. These results show that substrate binding triggers a conformational change in 12S, whereas product binding does not. The conformational change involves an increase in the amount of α-helix since markers for this secondary structure are prominent in the difference spectra of the substrate complex. The number of MM-CoA ligands bound per 12S hexamer can be gauged from the intensity of the MM-CoA Raman features and the fact that the protein concentration in the crystals is known from X-ray crystallographic data. Most crystal samples had six MM-CoAs per hexamer although a few, from different soaking experiments, contained only 1−2. However, both sets of crystals showed the same degree of protein conformational change, indicating that the change induced by the substrate is cooperative. This effect allowed us to record the Raman spectrum of bound MM-CoA without interference from protein modes; the Raman spectrum of a 12S crystal containing 2 MM-CoA ligands per hexamer was subtracted from the Raman spectrum of a 12S crystal containing six MM-CoA ligands per hexamer. The conformational change is reversible and can be controlled by soaking out or soaking in the ligand, using either concentrated ammonium sulfate solutions or the solution used in the crystallization trials. Malonyl-CoA also binds to 12S crystals and brings about conformational changes identical to those seen for MM-CoA; in addition, butyryl-CoA binds and behaves in a manner similar to propionyl-CoA. These data implicate the $-COO^-$ group on MM-CoA (that is transferred to biotin in the reaction on the intact enzyme) as the agent bringing about the cooperative conformational change in 12S.

Transcarboxylase (TC),[1] an enzyme complex produced by the anaerobic bacterium *P. shermanii*, catalyzes the reversible transfer of a carboxylate group from methylmalonyl-CoA (MM-CoA) to pyruvate, generating propionyl-CoA and

† This work was supported by a NIH grand to P. R. C. (DK 053053) and a NSF grand to V. C. Y. (MCB 0077488).

* To whom correspondence should be addressed. Phone: 216-368-0031. Fax: 216-368-3419. E-mail: carey@biochemistry.cwru.edu.

‡ Department of Biochemistry, Case Western Reserve University.

§ Department of Pharmacology, Case Western Reserve University, and Learner Research Institute, Cleveland Clinic Foundation.

10.1021/bi020422g CCC: $22.00
Published on Web 08/10/2002

oxaloacetate (*1*). The transfer occurs in two steps on two separate subunits of TC known as the 12S and 5S subunits:

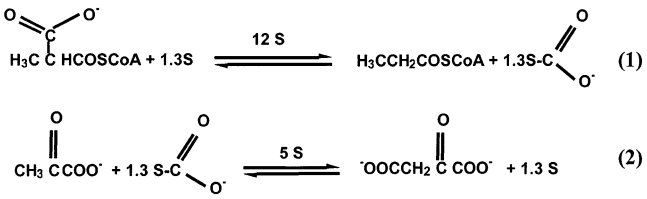

The half reactions shown above are similar to those occurring in important mammalian biotin-dependent carboxylases that catalyze key steps in several metabolic pathways, including fatty acid biosynthesis, gluconeogenesis, and amino acid catabolism. Not only does TC serve as a model system for its complex mammalian counterparts, but it also has the advantage of being modular. Overall, TC is a 1200 kDa complex composed of 30 polypeptides of three types: a central hexameric 12S subunit, six dimeric 5S subunits, and 12 1.3S biotinylated linkers (*2*, *3*). These subunits can be isolated from native TC or from cloned material, and to a degree they can be reassembled to form the holo enzyme. Importantly, the chemistries of the above half reactions can be studied independently using the individual subunits. Thus, in the present work we study the binding of the substrate MM-CoA to its cognate subunit 12S.

Using photoaffinity labeling Wood and colleagues showed that the isolated 12S subunit in solution binds up to six molecules of MM-CoA (*4*). In the absence of TC's other subunits, this complex is stable. Recently, we have solved the structure of MM-CoA bound to the 12S by X-ray crystallography (ref *5*, and unpublished work this laboratory) and confirmed that indeed six ligand molecules are bound per hexamer. A cartoon of the structure (Figure 1) shows that the hexamer is doughnut-shaped. It is made up of a dimer of trimers, and the MM-CoAs bind around the equator of the doughnut. A detailed description at the molecular level will be published shortly, upon completion of the refinement and fitting of the X-ray data. Raman spectroscopy provides information that complements that gained by crystallography—for example, on the strength of interactions in the active site and on details of electron distribution in some bonds. The 12S hexamer has a molecular weight of 338 000 Da, and until recently it would have been considered an impossible target for Raman analysis. However, we now show that high quality Raman data can be obtained from single crystals of 12S that have the potential to provide unique insights into the chemistry of the bound substrate and the conformational changes in 12S that accompany substrate binding.

Due to factors such as high protein to solvent water ratios and minimal interference from "background" signals, we have been able to show recently that single protein crystals provide Raman data that often could not be obtained in solution (*6*). The data are recorded using a Raman microscope (*7*) from crystals under growth conditions in hanging drops. Essentially the crystals are viewed using an optical

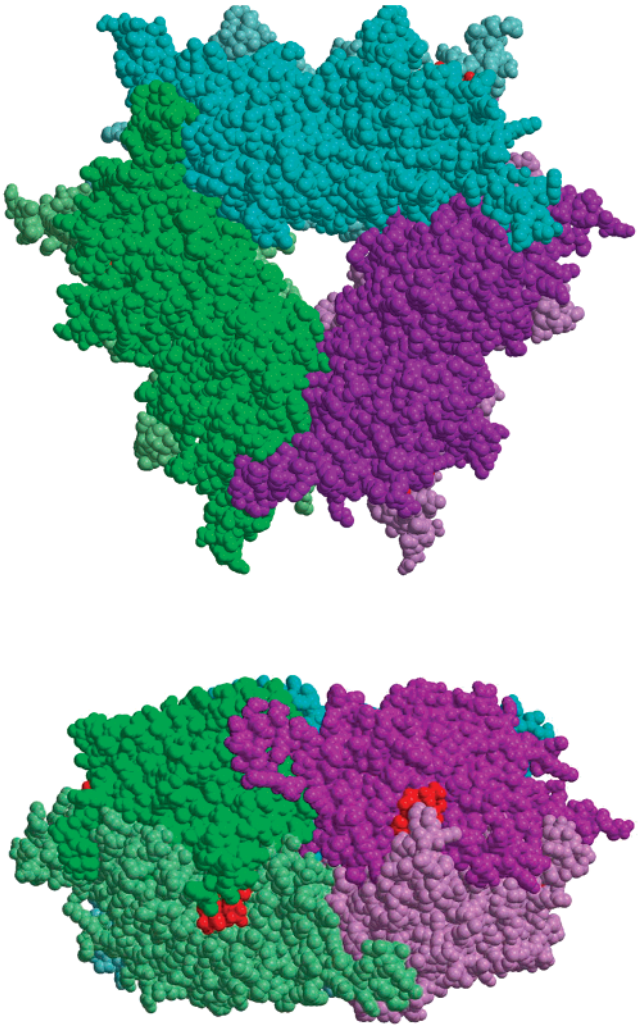

FIGURE 1: Plan and side view of the12S hexamer complexed with MMCoA. The MMCoA is shown in red. The images were generated using MOLSCRIPT (13) and Raster3D (14).

microscope; a laser beam travels on the optic axis of the microscope and, using a video camera attachment, can be seen focused on the target crystal. The microscope objective also collects the backscattered light, which is sent to a Raman spectrograph to yield the spectrum from the laser focal point on the crystal. Protein−ligand complexes are examined using Raman difference spectroscopy; the Raman spectrum of an apo crystal is subtracted from that of a crystal containing bound ligand. The resulting difference spectrum shows the Raman spectrum of the bound ligand with the possibility of the appearance of "positive" and "negative" peaks due to protein peptide and side-chain modes. Protein peaks occur when ligand binding perturbs the protein conformation; then "protein spectrum minus protein spectrum" does not subtract to zero in the difference spectrum. Thus, the Raman difference spectrum is a rich source of information on the conformation, interactions, and changes in electron densities for parts of the substrate as well as for parts of the enzyme. Difference spectra were obtained using crystals formed by cocrystallizing 12S and substrate as well as from crystals that had ligand repeatedly "soaked in" and "soaked out". The latter regime provides some control over the number of substrates bound per hexamer and can be used to characterize substrate-induced enzyme cooperativity.

[1] Abbreviations: TC, Transcarboxylase; CoA, coenzyme A; MM-CoA, methylmalonyl-CoA; M-CoA, malonyl-CoA.; Pr-CoA, propionyl-CoA.; Bu-CoA, butyryl-CoA; DTT, 1,4-dithiothreitol; Hepes, N-(2-hydroxyethyl) piperzine-N′-2-ethanesulfonic acid; PEG 4K, poly(ethylene glycol) 4000; MPD, 2,4-methylpentanediol; Ad, adenine.

MATERIALS AND METHODS

Enzyme and substrate samples. MM-CoA, M-CoA, Pr-CoA, and Bu-CoA were purchased from Sigma and dissolved in MilliQ water at a concentration of 100 mM. The substrate solutions were filtered (0.22 μm membrane) before the Raman spectra were collected. The 12S subunit of TC cloned from *P. shermanii* (strain 33 acquired from ATCC) was expressed in *Escherichia coli* strain JM109 and purified as described previously (*8*). Typically, 30 mg of high-purity 12S can be obtained from 30 g of cells. The protein was identified as having 524 amino acids (per monomer) with a MW $\sim$ 56 403 Da. (*10*). The specific activity of our purified 12S is 14.6 μmol/min/mg compared with the literature value of 13.4 μmol/min/mg (*9*).

Preparation of crystal complexes. Two approaches were used to obtain the ligand−crystal complexes: cocrystallization and the "soak-in" method. Prior to crystallization, the purified 12S was dialyzed against 20 mM potassium phosphate (pH 6.5) buffer containing 1 mM DTT and then concentrated to 10 mg/mL. To form the 12S−substrate complex, the concentrated 12S was incubated with 5 mM substrate overnight at 277 K. Crystallization was carried out at 293 K using the sitting-drop vapor-diffusion method. The growth of apo 12S or 12S/MM-CoA crystals was based on the conditions reported previously (*5*). Apo 12S crystals were grown from 0.1 M Hepes, pH 7.5, and 30−31% of 2,4-methylpentanediol (MPD). 12S−MM-CoA and 12S−M-CoA crystals were grown from 0.1 M sodium acetate pH 4.5 and 20−25% MPD.

Complex crystals of the 12S/Pr-CoA were grown from 0.2 M KH_2PO_4 and 10% PEG 4K. 12S/Bu-CoA crystals were grown from 0.1M sodium acetate pH 4.5 and 3−6% PEG 4K. For all 12S−substrate cocrystallizations, 5 mM $CdCl_2$ was added to make the crystals survive longer. Crystals with dimensions of approximately 0.2 $\times$ 0.2 $\times$ 0.2 mm^3 grew within 1 week.

Before recording Raman spectra, the crystals were transferred from sitting drops to hanging drops using cryoloops or a microspatula. The surfaces of the crystals were kept clean to minimize the Raman spectral baseline. Ligand−crystal complexes also can be formed by the soaking-in/soaking-out method. To incorporate ligands into apo 12S crystals, stock solutions of ligands were added to the hanging drop (8−10 μL clean well solution or 60 % ammonium sulfate) to make up to a final concentration of 5 mM. Soaking-in experiments normally required 60 min and soaking-out experiments could be carried out in 30 min at room temperature. Longer times may be used to completely fill or empty the six binding sites on each hexamer.

Raman spectroscopy of aqueous ligands. Raman spectra of the substrates (MM-CoA, M-CoA, Pr-CoA, and Bu-CoA) in solution were acquired by using 1,000 mW 647-nm laser excitation from an Innova 400 krypton laser (Coherent Radiation, Palo Alto, CA) and a modified Holospec f/1.4 axial transmission spectrometer (*11*). The concentrations of substrates were 3.5 mM in 50 μL sample volume. All spectra were recorded at room temperature with a total data collection time of 5 min. The computer subtraction was performed with GRAMS/32 software (Galactic Industries Company, Salem, NH).

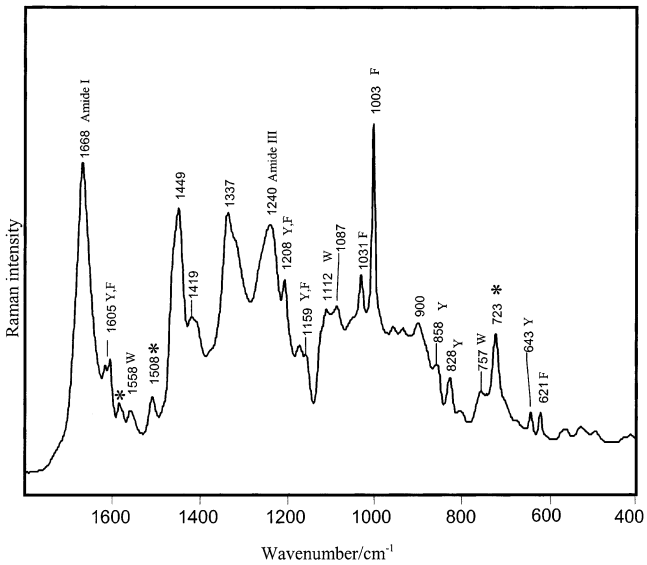

FIGURE 2: Raman spectrum of a single crystal of 12S with six molecules of propionyl-CoA bound per hexamer. Peaks due to the substrate are marked with an asterisk.

Raman spectroscopy of single crystals. Raman spectra of single crystals in situ (i.e., in hanging drops within crystallization trays) were acquired by using a HoloLab Series 500 Raman microscope (Kaiser Opitical Systems) interfaced with fiberoptics to the Holospec spectrometer (*7*). The 647 nm laser light was injected into the microscope's HoloProbe by using an optical fiber mounted on a XYZ stage. A single crystal in a hanging drop, within the growth tray, was placed on the microscope stage and viewed by using a charge-coupled device video camera incorporated into the microscope. The sample was excited with $\sim$100 mW 647 nm laser light, and 180° backscattered Raman light was collected from the protein crystal by using the long focal-length $\times$20 microscope objective lens. The Raman microscope also was calibrated by using standardized neon and tungsten lamps as described for the Holospec f/1.4 spectrometer (*7*). Computer subtraction, to obtain Raman difference spectra, was performed using the sharp phenylalanine band at 1003 cm^{-1} as an internal standard. The subtraction scale factor was adjusted to eliminate the contribution of the Phe band in the resultant spectrum.

Two methods were used to quantify the number of MM-CoA ligands bound to a single hexamer. In the first, apo crystal that had been soaked in 5 mM MM-CoA for several days were presumed to have six ligands bound per hexamer. Then the resulting ratio of the CoA peaks at 1508 or 723 cm^{-1} (Figure 2) to the protein CH_2 modes at 1449 cm^{-1} was taken as the standard value for six MM-CoA molecules per 12S hexamer. Alternatively, we measured different MM-CoA concentrations under the Raman microscope and generated a straight line relationship for intensity of the MM-CoA Raman modes as a function of concentration. This relationship was used to estimate the absolute concentration of MM-CoA in a protein crystal. The protein concentration in the crystal was calculated from X-ray data allowing us to calculate the number of MM-CoA per 12S hexamer. Applied to the same crystals, these two methods gave the same MM-CoA/hexamer ratio to within $\pm$10%.

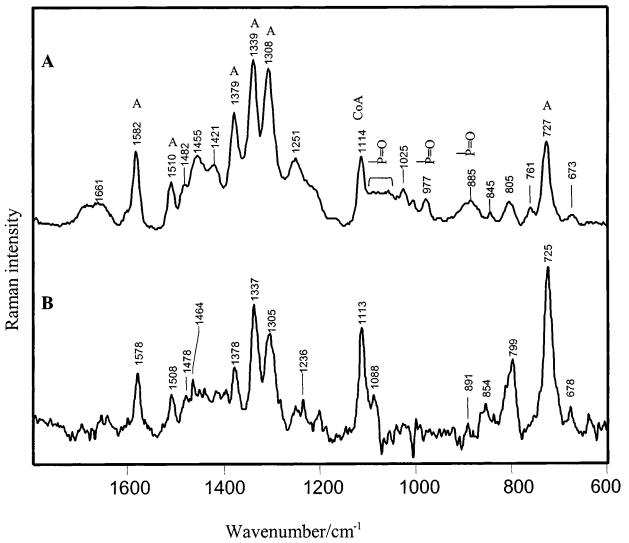

FIGURE 3: Raman difference spectra of propionyl-CoA. A, [3.5 mM propionyl-CoA in water] minus [water]. B, [propionyl-CoA bound to a single crystal of 12S] minus [apo crystal]. A = adenine ring mode, P═O phosphate mode, CoA unassigned mode from CoA.

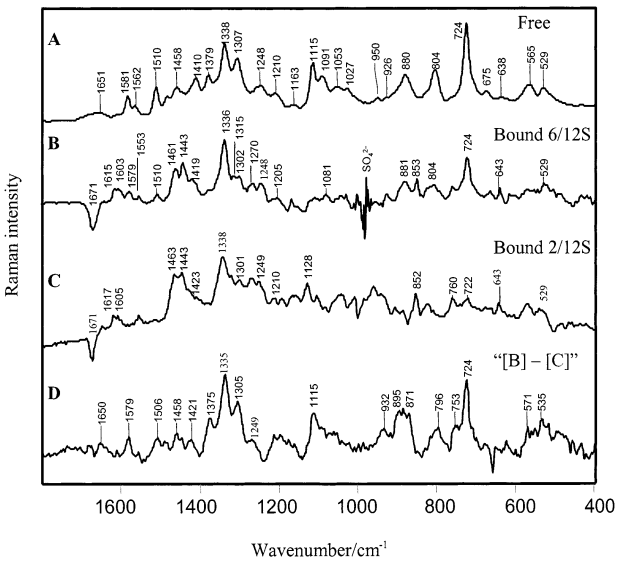

FIGURE 4: Raman difference spectra of methylmalonyl-CoA. A, [3.5 mM MMCoA in water] minus [water]; B, [MMCoA bound to a single crystal of 12S, 6 molecules substrate per hexamer] − [apo crystal]; C, [MMCoA bound to a single crystal of 12S, 2 molecules substrate per hexamer] − [apo crystal]; D, MMCoA bound to a single crystal of 12S, obtained by subtracting [2MMCoA-12S] from [6MMCoA−12S]. These spectra were generated from the same crystal by a soaking out experiment. Note: the derivative feature near 980 cm^{-1} in Figure 4B is due to the presence of sulfate anions.

RESULTS AND DISCUSSION

The binding of Pr-CoA and Bu-CoA to the 12S hexamer is discussed first because the Raman difference spectra are dominanted by Raman modes from the ligands. This provides a basis for the next topic, the binding of MM-coA and M-CoA to 12S, where interpretation is made more complex by the presence of many protein-base features.

Binding propionyl-CoA (Pr-CoA) and butyryl-CoA (Bu-CoA) to 12S crystals. The Raman spectrum of a single crystal of a 12S−Pr-CoA complex and band assignments are shown in Figure 2. The data are of high quality with a S/N ratio of 250/1. Apart from the minor bands due to Pr-CoA, the spectrum in Figure 2 is identical to that of the apo 12S hexamer. The positions of the amide I and III features at 1668 and 1240 cm^{-1} suggest that the 12S protein has a significant amount of β-sheet structure. The bound ligand makes clearly discernible contributions near 1580, 1508, and 723 cm^{-1}, which are marked by asterisks. The spectrum of free Pr-CoA is compared in Figure 3 with bound Pr-CoA obtained from the difference Raman spectrum [12S + Pr-CoA] minus [apo 12S]. The assignments of the Pr-CoA Raman modes given alongside the corresponding peaks in Figure 3A indicate that the Raman spectrum is dominated by CoA's adenine ring modes. This is due to the fact that adenine is a strong photon scatterer. The ligand bands identified in Figure 2 are from three such adenine modes. In addition, in Figure 3A,B, features near 880, 980, and the broad band near 1070−80 cm^{-1} likely originate from the modes due to the three phosphate groups on CoA. As our understanding for these modes improves the changes in the profiles upon binding will be a future source of additional structural information. The major features in the Raman difference spectrum, Figure 3B, are due to Pr-CoA "adenine" modes that have undergone minor frequency shifts due to contacts with the protein. A concentration 5 mM Pr-CoA is present in the mother liquor surrounding the crystal; however, concentrations at this level cannot detected by the Raman microscope. Thus, only crystal-bound Pr-CoA is seen in the spectrum shown in Figure 3B. Although no major protein features appear in the difference spectrum in Figure 3B, there is at least one minor protein band—the differential-type doublet seen at 1667−1680 cm^{-1} is assigned to an amide I band from a very minor conformational change in the peptide backbone caused by ligand binding.

The Raman difference spectrum in Figure 3B was obtained by soaking Pr-CoA into a single crystal of 12S for 60 min to form the enzyme−substrate complex; similar results were obtained for a soak of 10 min. In addition, analogous results were obtained for "soaking in" Bu-CoA (data not shown). However, 12S−Pr-CoA complexes formed by cocrystallization gave quite different results. Marked differences are observed—for example, in the position and intensity profile of the "adenine triplet" near 1340 cm^{-1} and the intensity of the band at 1580 cm^{-1} (data not shown). Wood and colleagues observed that Pr-CoA is hydrolyzed slowly when in contact with 12S (*4*). Thus, it is likely that the Pr-CoA is hydrolyzed completely during the 5−6 days it takes to grow single crystals by cocrystallization and that the difference spectra represent just CoA bound to 12S. During the soaking-in experiments, there is insufficient time for significant Pr-CoA hydrolysis to occur, and this approach thus provides the only means of studying intact Pr-CoA bound to 12S.

Binding methylmalonyl-CoA (MM-CoA) and malonyl-CoA (M-CoA) to 12S crystals brings about a change in protein conformation. The contrast between the Raman difference spectra of Pr-CoA bound to 12S (Figure 3B) and MM-CoA bound to 12S (Figure 4B) is striking. Whereas the difference spectrum of the Pr-CoA complex shows almost only Pr-CoA modes, the difference spectrum involving MM-CoA in Figure 4B has a rich assortment of "positive" and "negative" features, only a few of which can be assigned to MM-CoA. This is obvious from a rapid comparison of the difference spectrum of the complex in Figure 4B with that for free MM-

Table 1: Band Assignments for Raman Difference Spectra: MMCoA- and MCoA-Bound 12S Single Crystals (Frequencies in cm^{-1})

MMCo	MCoA	assignments
1671	1668	amide I
1615	1617	Y
1607	1607	F
1579	−	CoA (Ad)
1553	1553	W
1510	1507	CoA (Ad)
1461	1463	CH_2 scissor (CH_2, CH_3 def.)
1443	1443	CH_2 scissor (CH_2, CH_3 def.)
1419	1419	(MM)-COO^- symmetric stretch
1336	1341	α-helix, CH_2 twist wag (Ad, CoA)
1315	1315	CH_2 twist wag
1302	1301	CoA (Ad)
1270	1270	amide III, α-helix
1249	1249	amide III, disordered
1205	1208	Y, F
1081	1078	P═O, CoA
881	882	P═O, CoA
853	851	Y
759	758	V
724	720	CoA (Ad)
643	642	Y
529	523	amide IV, α-helix

CoA in Figure 4A. In Figure 4B adenine modes (from MM-CoA) can only be assigned with confidence to peaks at 724, 1510, and 1579 cm^{-1}, with the likelihood that the feature at 1336 cm^{-1} also contains a contribution from an adenine mode. In addition, modes associated with CoA's phosphate group may appear. Many of the features in Figure 4B can be assigned to aromatic amino acid side chain modes and peptide vibrations. Assignments of all the peaks identified are given in Table 1, which also lists the features seen in the Raman difference spectrum of the complex between 12S and malonyl-CoA (M-CoA). The difference spectrum for MM-CoA and M-CoA binding to 12S are essentially superimpossible (data not shown), demonstrating the highly reproducible nature of the Raman difference data.

A key conclusion from Figure 4B is that 12S undergoes a conformational change upon MM-CoA binding. As a result, characteristic α-helix marker bands appear at 1336, 1270, and (tentatively) 529 cm^{-1} (these assignments are based on literature values (*12*) and unpublished work in this laboratory). The band near 1336 cm^{-1} has little or no contribution from the ligand since in Figure 4C the intense CoA mode near 725 cm^{-1} is missing. There is a relatively intense negative band near 1671 cm^{-1}, in a region where either *β*-sheet or random coil structure may make a contribution. Taken together, these data demonstrate that upon MM-CoA binding to 12S crystals, the protein undergoes an overall increase in α-helical structure with a concomitant loss of random coil or *β*-sheet. Although exact quantitation is difficult, the area under the negative 1671 cm^{-1} feature in Figure 4B is ∼6% of that under the amide I feature seen in Figure 2. Therefore, we conclude that the change in secondary structure involves a few percent of the peptide bonds in the whole protein. It is pertinent to note that the conformational change we are observing appears to be independent of the medium surrounding the crystal since identical results were obtained for 12S crystals that undergo ligand "soaking in " and "soaking out" in a solution used for the crystallization trials or in concentrated ammonium sulfate. However, the intense sulfate band near 980 cm^{-1} is difficult to subtract to zero in the difference spectrum and gives rise to the derivative feature seen in Figure 4B.

Several features due to aromatic side chains of 12S also demonstrate that the environments of some of 12S's aromatic residues are perturbed by substrate binding (Table 1). Although the aromatic side chains give rise to weak features in the difference spectrum, the features are completely reproducible from experiment to experiment. Their appearance could be a consequence of the change in secondary structure discussed above. An additional factor is that parts of the CoA may bind close to aromatic side chains and exclude water molecules, bringing about an increase in the Raman cross section for those entities.

Evidence for cooperativity. The evidence for a cooperative change in the 12S structure upon binding one or two MM-CoA ligands per 12S hexamer is apparent from the comparison of the difference Raman spectra for [hexamer + 6 MM-CoAs] − [hexamer] and [hexamer + 2 MMCoAs] − [hexamer], panels B and C, respectively, of Figure 4. The methods used to quantitate the number of ligands bound is given in Materials and Methods. The higher number of MM-CoAs bound in Figure 4B is apparent by the increased intensities at 724, 804, 1336, 1510, and 1579 cm^{-1} due to CoA's adenine group. The salient feature from Figure 4B,C is that the changes to the protein's aromatic side chain features and secondary structure—notably, the "negative" amide I band at 1671 cm^{-1},— are essentially identical. Thus, two ligands bound to a single hexamer bring about the same degree of change as six, providing strong evidence for a cooperative change when only a fraction of the hexamer's six binding sites are occupied. Titration experiments leading to a more quantitative description are in progress.

Using the cooperative effect to obtain the Raman difference spectrum of bound MM-CoA. The Raman difference spectra shown in Figure 4B,C are dominated by features arising from the protein's conformational change caused by ligand binding. However, the cooperativity effect described above suggests a facile means of obtaining the spectrum of the bound ligand uncluttered by interfering protein modes. Since the changes in protein conformation brought about by two or six ligands binding to a single hexamer appear to be the same, a simple subtraction [hexamer + 6 MM-CoAs] − [hexamer + 2 MM-CoAs] will yield the "clean" spectrum of bound MM-CoA. The resulting trace is shown in Figure 4D: it resembles the spectrum of "free" MM-CoA with minor differences and is quite distinct from the protein-dominated Figure 4B,C. There are small but significant shifts in adenine ring mode positions between panels A and D of Figure 4, as well as changes in the relative intensity pattern that reflect adenine−12S contacts.

One notable difference feature involves the peak seen from the unbound substrate at 1410 cm^{-1} (Figure 4A). This peak is not detectable in the spectrum of Pr-CoA (Figure 3A) and in fact represents one of the major differences between Figures 3A and 4A. It is assigned to the symmetric stretch of MM's $-COO^-$ group, which is of course absent in Pr-CoA. It appears to shift to 1421 cm^{-1} when bound to 12S (Figure 4D). These assignments will be confirmed in future experiments by isotopic substitutions in the $-COO^-$ group. The potential identification of this mode for the bound substrate holds high promise for providing insight into the chemistry of the $-COO^-$ group as it is being prepared for

transfer to biotin's ureido ring. The present finding, that this key group appears to trigger the observed cooperative conformational change in the 12S hexamer, serves to heighten the interest in the details of the interaction between 12S and its substrate's $-COO^-$ group.

REFERENCES

1. Wood, H. G., and Zwolinski, G. K. (1976) *CRC Crit. Rev. Biochem. 4*, 47−122.
2. Wood, H. G. (1979) *CRC Crit. Rev. Biochem. 7*, 143−160.
3. Wood, H. G., and Kumar, G. K. (1985) *Ann. N.Y. Acad. Sci. 447*, 1−21.
4. Wood, H. G., and Poto, E. M. (1978) *J. Biol. Chem. 253*, 2979−2983.
5. Wang, Y., Hyatt, D. C., Rivera, R. E., Carey, P. R., and Yee, V. C. (2001) *Acta Crystallogr., Sect. D 57*, 266−268.
6. Dong, J., Swift, K., Matayoshi, E., Nienaber, V. L., Weitzberg, M., Rockway, T., and Carey, P. R. (2001) *Biochemistry 40*, 9751−9757.
7. Dong, J., Wan, Z. L., Chu, Y. C., Nakagawa, S. N., Katsoyannis, P. G., Weiss, M. A., and Carey, P. R. (2001) *J. Am. Chem. Soc. 123*, 7919−7920.
8. Altose, M. D., Zheng, Y., Dong, J., Palfey, B., and Carey, P. R. (2001) *Proc. Natl. Acad. Sci. U.S.A. 98*, 3006−3011.
9. Thornton, C. G., Kumar, G. K., Haase, F. C., Phillips, F. B., Woo, S. B., Park, V. M., Magner, W. J., Shenoy, B. C., Wood, H. G., and Samols, D. (1993) *J. Bacteriol. 175*, 5301−5308.
10. Woo, S. B., Shenoy, B. C., Wood, H. G., Magner, W. J., Kumar, G. K., Beegen, H., and Samols, D. (1993) *J. Biol. Chem. 268*, 16413−16419.
11. Rivera, R. E. (2001) Ph.D. Thesis, Case Western Reserve University, Cleveland.
12. Dong, J., Dinakarpandian, D., and Carey, P. R. (1998) *Appl. Spectrosc. 52*, 1117−1122.
13. Overman, S. A., and Thomas, G. J., Jr. (1998). *Biochemistry 37*, 5654−5665.
14. Kraulis, P. J., *J.* Appl. *Cryst. 24*, 946−950.
15. Merritt, E. A., and Bacon, D. J. *Methods Enzymol. 277*, 505−524.

BI020422G